Pakistan Veterinary Journal

ISSN: 0253-8318 (PRINT), 2074-7764 (ONLINE)
DOI: 10.29261/pakvetj/2026.026

RESEARCH ARTICLE

Mechanistic Study of cGAS-STING Pathway–Induced Pyroptosis in Corneal Epithelial Cells in Keratoconjunctivitis Sicca

Haishu Dong[1], Jiawei Chen[4], Jian Sun[2], Muhammad Tariq[3], Zipei Jiang[1*] and Jiayu Zhang[4*]

[1]Department of Ophthalmology, The First Affiliated Hospital of Wenzhou Medical University, Wenzhou, Zhejiang, 325000, China; [2]College of Veterinary Medicine, Yunnan Agricultural University, Kunming 650201, China; [3]College of Animal Science and Technology, Nanjing Agricultural University, Nanjing, Jiangsu, 210095, China; [4]Department of Ophthalmology, The Third Affiliated Hospital of Wenzhou Medical University, Ruian, Zhejiang, 325200, China.
*Corresponding author: jzp20012000@163.com (ZJ); zhangjiayu0201@wmu.edu.cn (JZ)

ARTICLE HISTORY (25-1218)

Received: December 13, 2025
Revised: February 08, 2026
Accepted: February 14, 2026
Published online: February 19, 2026

Key words:
cGAS–STING pathway
Cornea epithelial cells
Pyroptosis
Inflammatory response
Keratoconjunctivitis sicca

ABSTRACT

Xerophthalmia, also called Keratoconjunctivitis sicca (KCS), is often referred to as dry eye disease (DED). It is a chronic immune-mediated ocular surface inflammatory disease. Its characteristics are corneal epithelial cell damage and persistent local inflammation. Increasing evidence indicates that pyroptotic death of corneal epithelial cells can significantly exacerbate tissue damage and accelerate disease progression. The cyclic guanosine monophosphate-adenosine monophosphate synthase-interferon gene stimulator protein (cGAS–STING) pathway is a key DNA-sensing signaling pathway in inflammatory cell death; however, its role in KCS is unclear. In this study, a KCS murine model was constructed in C57BL/6 mice, and different concentrations of H151 (a selective cGAS–STING inhibitor) were used for treatment. Human corneal epithelial cells (HCECs) were placed in an in vitro environment, first exposed to a hypertonic condition, and then treated with H151. The activity of the cGAS-STING pathway, pyroptosis, and the inflammatory response were evaluated by measuring tear secretion, performing TUNEL staining, using CCK-8, measuring LDH release, and using Western blotting (WB). In the DED mouse model, tear secretion decreased, corneal inflammatory cytokine expression increased, and cGAS–STING–related proteins were upregulated. Using H151 could significantly improve tear secretion, reduce pathological activity, and also reduce the quantity of TUNEL-positive cells and the level of caspase-3 and gasdermin E in a manner dependent on the dose. Similar to the in vivo experimental results, hypertonic stress activated the cGAS–STING pathway in HCECs, as evidenced by decreased cell viability, increased LDH release, and increased pyroptosis. H151 can enhance cell viability and inhibit the pyroptosis-related signaling pathway to alleviate these effects. The research results indicate that the cGAS–STING pathway is involved in the pyroptosis of corneal epithelial cells in Sjögren's syndrome and is closely associated with caspase-3/GSDME signaling. These findings suggest that cGAS–STING activation may contribute to pyroptotic processes rather than directly initiating caspase-3/GSDME-mediated pyroptosis. Accordingly, this pathway may represent a potential therapeutic target for DED.

To Cite This Article: Dong H, Chen J, Sun J, Tariq M, Jiang Z and Zhang J, 2026. Mechanistic study of cGAS-STING pathway–induced pyroptosis in corneal epithelial cells in keratoconjunctivitis Sicca. Pak Vet J, 46(2): 361-372. http://dx.doi.org/10.29261/pakvetj/2026.026

INTRODUCTION

Keratoconjunctivitis sicca (KCS), also known as dry eye disease (DED) in humans, is a multifactorial disease characterized by tear film instability and loss of ocular surface homeostasis. In veterinary medicine, KCS primarily occurs in dogs and is rare in cats (Avci *et al*., 2025; Çaki and Durmuş, 2025). KCS pathology is related to slow inflammation and the gradual damage of corneal and conjunctival epithelial layers (Song *et al*., 2024; Roszkowska *et al*., 2025). Clinical patients will have symptoms such as dry eyes, irritation, burning pain, and changes or blurring of vision. If regular treatment is not carried out, the disease will cause injury to the corneal

epithelium, and severe cases will lead to permanent loss of vision (Shimizu *et al*., 2021; Hu *et al*., 2025). Over the past several decades, the incidence of KCS/DED worldwide has increased, partly due to population aging, increased screen time, and greater environmental pressure. Therefore, DED represents a common ocular surface disorder and an increasingly serious public health concern (Al-Mohtaseb *et al*., 2021; Papas *et al*., 2021).

The corneal epithelium is the primary barrier of the ocular surface and is extremely important for the stability of the tear film and normal vision (Kontoh-Twumasi *et al*., 2025). The loss of epithelial integrity during the progression of KCS or DED is widely recognized as a key catalyst for the inflammatory cascade and ocular surface dysfunction (Li *et al*., 2024). Early studies predominantly focused on apoptosis and necrotic cell death; however, subsequent investigations have increasingly focused on pyroptosis, a unique form of regulated cell death (Zhong *et al*., 2023). Pyroptosis is mediated by Gasdermin proteins, and the cells will appear swollen, plasma membrane pores will form, and pro-inflammatory cytokines, for example interleukin-1β (IL-1β) and interleukin-18 (IL-18) will be released, which makes the ocular surface inflammation more severe (Fischer *et al*., 2021). More and more evidence suggests that corneal epithelial cell pyroptosis may cause tissue damage in KCS (Liao *et al*., 2024). Despite advances in research, the molecular events controlling corneal epithelial pyroptosis remain unclear, especially regarding the possible involvement of the cyclic GMP–AMP synthase (cGAS) stimulator of interferon genes (STING) pathway.

In recent years, the cGAS–STING signaling pathway has been increasingly studied in the research of immune response in animals and humans (Yang *et al*., 2022). This pathway is a cytosolic deoxyribonucleic acid (DNA) sensor, which can detect abnormal intracellular DNA, such as damaged mitochondrial DNA, translocated nuclear DNA, and DNA from pathogens (Han *et al*., 2024). After DNA is recognized, cGAS generates cyclic guanosine monophosphate–adenosine monophosphate (cGAMP), cGAMP activates STING, initiates downstream pathways, and then type I interferons together with pro-inflammatory cytokines are generated, triggering the innate immune response (Qian *et al*., 2025). The dysregulation of the cGAS–STING pathway is not only related to antiviral and anti-tumor but also to various inflammations and autoimmune diseases, including conditions such as systemic lupus erythematosus, Sjögren's syndrome, and psoriasis (Xu *et al*., 2023; Gu *et al*., 2024; Zhang *et al*., 2025). Activation of the pathway enhances the production of pro-inflammatory mediators, for example, CXC motif chemokine ligand 10 (CXCL10), interleukin-6 (IL-6), and interferon-β (IFN-β) (Ouyang *et al*., 2023), and the levels of these mediators are elevated in DED and KCS models (Almulhim *et al*., 2024). More and more research shows that excessive activation of the cGAS–STING pathway may make corneal epithelial injury more serious, exacerbate inflammation, and increase the number of cell deaths; drug targeting can protect cells from oxidative stress and reduce cell deaths (Ouyang *et al*., 2023). These results indicate that cGAS–STING signaling could be a key contributor to the pathogenesis of KCS, and it is necessary to explore the effect on corneal epithelial cell apoptosis.

We use the mouse model of keratoconjunctivitis sicca induced by scopolamine hydrobromide and the in vitro hyperosmotic stress model of HCECs to explore the function of the cGAS–STING pathway in disease development. It is particularly important to determine how this signaling axis regulates corneal epithelial cell pyroptosis and the production of inflammatory cytokines. This strategy notes that the cGAS–STING signaling pathway in corneal epithelial cells triggers pyroptosis in KCS and explores therapeutic targets.

MATERIALS AND METHODS

DED Mouse Model and Drug Intervention: A total of 30 female C57BL/6 mice, 6-8 weeks old, were obtained from Beijing Vital River Laboratory Animal Technology Co., Ltd. After 1 week of adaptation, the DED model was induced by placing the mice in a dry environment and subcutaneously injecting scopolamine hydrobromide (0.6mg/250μL; hy-n0296a, MedChem Express, Monmouth Junction, NJ, USA). As outlined earlier (Wang *et al*., 2025), four injections per day were performed for seven consecutive days. The mice were assigned randomly to five experimental groups: normal control (CT), DED model (DED), low-dose H151 intervention (DED+H151-L, 500nmoL/mouse), medium-dose H151 intervention (DED+H151-M, 750nmoL/mouse), and high-dose H151 intervention (DED+H151-H, 1000Nano Letters/mouse). Mice assigned to the intervention groups received intraperitoneal injections of the STING inhibitor H151 (HY-112693, MedChem Express, Monmouth Junction, NJ, USA) once daily for seven consecutive days, administered 1h before each scopolamine hydrobromide injection. The CT and DED groups received equal volumes of vehicle intraperitoneally. Following the completion of the experiment, the mice were humanely euthanized, and their eyes and corneal tissues were harvested for subsequent analyses.

Tear Secretion Measurement: At 1.5h after scopolamine injection, a cotton thread soaked with phenol red was inserted into the conjunctival sac and maintained for 1 min. The wetted length of the thread was measured. A wetting length of less than 2mm indicated that the scopolamine dose effectively reduced tear secretion and was suitable for subsequent experiments.

Cell Culture and Treatment: HCECs (JNO-H0616, Genio Biotech, Guangzhou, China) were cultured at 37°C with 5% CO_2 in DMEM/F12 medium (SNM-004B, SUNNCELL, Wuhan, China) supplemented with 10% fetal bovine serum (FBS, Thermo Fisher Scientific, USA). The cells were authenticated via STR profiling and verified to be free of mycoplasma.

For the *in vitro* KCS model, HCECs were exposed to hyperosmotic medium (312–500mOsm) (Wang *et al*., 2025). The cells were divided into the normal control (NC), hypertonic (HOP), and HOP+ cGAS/STING inhibitor (HOP+H151) groups. HOP cells grow in a medium with added NaCl (450mOsm), and NC cells grow in a normal osmotic pressure (310mOsm). The HOP + H151 group cells were exposed to a range of concentrations of STING inhibitor H151 (1, 2.5, or 5μM) for 24 hours before the experiment.

Cell Viability Assay: The cell counting kit-8 (CCK-8; FNCK064; FineTest, Wuhan, China) was used to assess cell viability and determine the impact of H151 on HCEC cell survival. The cells were plated into 96-well plates and were adherent 24 hours before H151 treatment. Each well was treated with 100μL, 10μL CCK-8, and incubated at 37°C for 2.5 hours. The absorbance at 450nm was measured with a microplate reader (Bertin Instruments, Burlington, VT, USA). Cells were assigned to the NC, HO, and HOP+H151 groups, and the HOP+H151 group was further subdivided into 1, 2.5, and 5μM to examine how cell viability varies with dose.

Cell Death Assay: HCEC apoptosis was assessed by quantifying lactate dehydrogenase (LDH) release. The cells (5×10^3 cells/well) were grown in 96-well plates. After the indicated treatments, the culture plates were centrifuged at 400 ×g for 5 min. Subsequently, 120μL of cell culture supernatant was collected and incubated with LDH reaction solution at room temperature for 30 min in the dark. The reaction was terminated using the stop solution, and absorbance was measured at 490nm with a microplate reader. LDH released was determined according to the supplied protocol of the LDH assay kit (JLCS1449, Gelatins, Shanghai, China).

Inflammatory Cytokine Measurement: ELISA was used to detect IL-6, tumor necrosis factor-alpha (TNF-α), and IL-1β levels in mouse corneal tissues and HCECs. Kits were purchased from Mibio (ml063159; ml002095; ml106733, Shanghai, China) and Beyotime (PI330; PT518; PI305, Shanghai, China), and all procedures were carried out following the manufacturers' protocols. Briefly, mouse corneal tissues were homogenized in ice-cold lysis buffer and centrifuged to collect supernatants, while culture supernatants from treated HCECs were collected directly. Samples and standards were added to precoated 96-well plates and incubated according to the manufacturer's instructions. After washing, biotin-conjugated detection antibodies and horseradish peroxidase-linked streptavidin were sequentially applied, followed by substrate solution incubation. The reaction was terminated with stop solution, and absorbance was measured at 450nm using a microplate reader. Cytokine concentrations were calculated from standard curves and normalized to total protein content where applicable.

Terminal deoxynucleotidyl transferase dUTP Nick-End Labeling (TUNEL) Assay for Apoptosis in Mouse Corneal Tissue and HCECs: After euthanasia, mouse eyeballs were fixed in FAS eyeball fixative (TT154, Huayueyang Biotech, Beijing, China), dehydrated, embedded in paraffin, sectioned, and deparaffinized. HCECs were seeded on coverslips and fixed with 4% paraformaldehyde (P0099, Beyotime, Shanghai, China) for 30 min. Samples were treated with DNase-free proteinase K for 20 minutes at room temperature, then rinsed with PBS (PB180327, Procell, Wuhan, China). The tissue sections were incubated with 3% hydrogen peroxide for 20 minutes to inhibit endogenous peroxidase activity. Tissues and cells were incubated with TUNEL working solution (C1088; C1090, Beyotime, Shanghai, China) at 37°C in darkness for 1 hour, washed with PBS, and stained with 4′,6-diamidino-2-phenylindole (DAPI, 40728ES03, YEASEN, Shanghai, China) for 5min. After the final PBS washes, samples were mounted and analyzed for apoptosis using a fluorescence microscope.

Western Blot (WB) Analysis: Total protein was isolated from mouse corneal tissues and HCECs using a radioimmunoprecipitation assay lysis buffer (PC101, YaYme, Shanghai, China). Protein concentrations were quantified, then resolved by sodium dodecyl sulfate–polyacrylamide gel electrophoresis and subsequently transferred onto polyvinylidene fluoride membranes. The membranes were blocked with 5% milk for 1 hour, after which they were incubated overnight at 4°C with the primary antibody cGAS (29958-1-AP, proteintech, Wuhan, China), TANK-Binding Kinase 1 (TBK1; 29958-1-AP; 67211-1-Ig, Proteintech, Wuhan, China), STING, phosphorylated interferon regulatory factor 3 (p-IRF3), IRF3, caspase-3, cleaved-caspase-3 (3337; 29047; 26306; 9662; 9661, Cell Signaling Technology, Danvers, MA, USA), p-TBK1, GSDME, gasdermin E n-terminal domain (GSDME-N), and beta-actin (β-actin; AF8190; DF9705; AF4016; AF7018, Affinity, Jiangsu, China). Membranes were then incubated for 1 hour with HRP-conjugated goat anti-rabbit secondary antibodies (A0208; A0352, Beyotime, Shanghai, China). The protein bands were detected with a chemiluminescence imaging system (Bio-Rad, California, USA) and quantified via ImageJ software, using β-actin as the loading control.

Quantitative Real-Time Polymerase Chain Reaction (qRT-PCR): Total RNA was isolated from mouse corneal tissues and HCECs with TRIzol reagent (R0016; Beyotime, Shanghai, China). RNA concentration and purity were assessed by spectrophotometry, and equal amounts of RNA were reverse-transcribed into cDNA using the Hifair® AdvanceFast First-Strand cDNA Synthesis Kit (11150ES60, YEASEN, Shanghai, China). qRT-PCR was carried out on an Mx3005P system (Agilent, Santa Clara, USA) using the Hifair® V Multiplex One Step RT-PCR Kit (13089ES60, YEASEN, Shanghai, China) with the following cycling conditions: initial denaturation at 95°C for 5 min, followed by 40 cycles of denaturation at 95°C for 10s and annealing/extension at 60°C for 30s. Expression levels of the genes were quantified using the 2^-ΔΔCt calculation and normalized to β-actin. The primer sequences are listed in Table 1.

Statistical Analysis: Statistical analyses were performed with GraphPad Prism 9.5 (GraphPad Software, La Jolla, CA, USA). Data are presented as mean ± standard deviation (SD). All Western blot and qRT-PCR experiments were performed using at least three independent biological replicates. Inter-group comparisons were made using one-way ANOVA followed by Tukey's post-hoc test, and a p-value <0.05 was considered statistically significant.

RESULTS

H151 Mitigates Corneal Inflammation and Enhances Tear Secretion in KCS or DED Mice via cGAS–STING Pathway Inhibition: Tear secretion measurement showed that tear secretion in DED mice was markedly decreased

compared with that in the CT group (P<0.05), suggesting that the model had been successfully established (Fig. 1A). Administration of the cGAS–STING inhibitor H151 could improve tear secretion in a dose-dependent manner. Compared with untreated DED mice, tear secretion in the DED+H151-H group increased the most (P<0.05; Fig. 1A). The measurement of IL-6, TNF-α, and IL-1β in corneal homogenate revealed a significant increase in the KCS/DED group compared with the CT group (P<0.05; Fig. 1B), reflecting a strong local inflammatory response. H151 intervention inhibited the upregulation of cytokines to different degrees, and the effect of DED+H151-H group was the best (P<0.05; Fig. 1B).

Table 1: Primer sequences for qRT-PCR

Gene Name	Species	Sequence (5′–3′)
IL-6	Human	F: AGACAGCCACTCACCTCTTCAG
		R: TTCTGCCAGTGCCTCTTTGCTG
IL-6	Mouse	F: TACCACTTCACAAGTCGGAGGC
		R: CTGCAAGTGCATCATCGTTGTTC
TNF-α	Human	F: CCAGGGACCTCTCTCTAATCA
		R: TCAGCTTGAGGGTTTGCTAC
TNF-α	Mouse	F: TCTTCTCATTCCTGCTTGTGG
		R: TCTGGGCCATAGAACTGATGA
IL-1β	Human	F: GTACCTGTCCTGCGTGTTGA
		R: GGGAACTGGGCAGACTCAAA
IL-1β	Mouse	F: GAAGCTGGATGCTCTCATCTG
		R: TTGACGGACCCCAAAAGAT
cGAS	Human	F: GGCCTGCGCATTCAAAACTG
		R: AGCCGCCATGTTTCTTCTTGG
cGAS	Mouse	F: TTCCACGAGGAAATCCGCTGAG
		R: CAGCAGGGCTTCCTGGTTTTTC
STING	Human	F: CCTGAGTCTCAGAACAACTGCC
		R: GGTCTTCAAGCTGCCCACAGTA
STING	Mouse	F: CGTGCTGGCATCAAGAATCG
		R: TCGAGACTCGGGGACATCTT
TBK1	Human	F: CAACCTGGAAGCGGCAGAGTTA
		R: ACCTGGAGATAATCTGCTGTCGA
TBK1	Mouse	F: GACATGCCTCTCTCCTGTAGTC
		R: GGTGAAGCACATCACTGGTCTC
IRF3	Human	F: TCTGCCCTCAACCGCAAAGAAG
		R: TACTGCCTCCACCATTGGTGTC
IRF3	Mouse	F: CGGAAAGAAGTGTTGCGGTTAGC
		R: CAGGCTGCTTTTGCCATTGGTG
Caspase-3	Human	F: GGAAGCGAATCAATGGACTCTGG
		R: GCATCGACATCTGTACCAGACC
Caspase-3	Mouse	F: GGAGTCTGACTGGAAAGCCGAA
		R: CTTCTGGCAAGCCATCTCCTCA
GSDME	Human	F: GATCTCTGAGCACATGCAGGTC
		R: GTTGGAGTCCTTGGTGACATTCC
GSDME	Mouse	F: ACGGACACCAATGTAGTGCTGG
		R: CTCTCATGCTCGAAGCCACCAT
β-actin	Human	F: GAGCTACGAGCTGCCTGACG
		R: GTAGTTTCGTGGATGCCACAG
β-actin	Mouse	F: CGTGAAAAGATGACCCAGATCA
		R: TGGTACGACCAGAGGCATACAG

WB analysis showed that, relative to CT mice, the expression levels of cGAS, STING, p-TBK1, and p-IRF3 in the DED group increased (P<0.05), and the overall protein levels of TBK1 and IRF3 remained constant (Fig. 1C). H151 treatment markedly suppressed the expression of those proteins (P<0.05; Fig. 1C). qRT-PCR analysis revealed that the mRNA levels of IL-6, TNF-α, IL-1β, cGAS, STING, TBK1 and IRF3 in the corneas of DED mice were markedly elevated than those in CT mice (P<0.05; Fig. 1D). The treatments with H151 at various doses significantly reduced the expressions of these genes, and the inhibition was the most obvious in the DED+H151-H group (P<0.05; Fig. 1D). KCS induces corneal epithelial inflammation and also activates the cGAS-STING pathway, which may be potentially linked to pyroptosis. Inhibition of the cGAS–STING pathway with H151 markedly reduced corneal inflammation and partially improved tear production, indicating a significant role for this signaling axis in the pathogenesis of KCS.

H151 Reduces Corneal Epithelial Pyroptosis in DED Mice by Inhibiting the cGAS–STING Pathway: TUNEL staining revealed significantly elevated numbers of DNA-fragmented corneal epithelial cells in the DED group relative to the CT group (P<0.05), consistent with pyroptosis-associated corneal epithelial cell damage in DED mice (Fig. 2A). After H151 treatment, the quantity of TUNEL-positive cells gradually decreased in a dose-dependent manner, with the DED + H151-H group exhibited the greatest improvement (P<0.05; Fig. 2A). WB analysis further showed that the levels of protein caspase-3, cleaved caspase-3, GSDME, and its active fragment GSDME-N were markedly increased in the DED group compared with CT mice (P<0.05). H151 intervention reduced the upregulation of these proteins in a dose-dependent fashion (Figs. 2B–2D). qRT-PCR analysis further demonstrated that *caspase-3 and GSDME* mRNA expression in KCS corneal tissues was markedly elevated compared with that in CT mice (P<0.05), and H151 administration led to a reduction in these levels, especially in the DED+H151-H group (P<0.05; Fig. 2E). The results indicated that activation of the cGAS–STING pathway contributed to corneal epithelial pyroptosis in KCS, and H151 treatment alleviated this effect by inhibiting pathway hyperactivation.

H151 Improves Viability and Suppresses Inflammatory Cytokine Expression in Hyperosmotic-Damaged Cells: Cell viability assay showed that H151 had no cytotoxicity at a concentration ≤5μM, whereas high doses (≤7.5μM) significantly reduced HCEC viability (P<0.05), indicating that concentrations up to 5μM were safe (Fig. 3A). The activity of HCEC in the HOP group was markedly reduced compared to the level in the NC group (P<0.05). Administration of H151 improved cell viability in a dose-dependent fashion, and the HOP+H151-H showed the most significant effect (P<0.05; Fig. 3B).

Compared with NC, HOP cells showed a markedly increased LDH release (P<0.05), and the administration of H151 attenuated this effect in a concentration-dependent fashion (P<0.05; Fig. 3C). ELISA analysis shows that the levels of IL-6, TNF-α, and IL-1β in HOP cells are significantly increased (P<0.05). After H151 treatment, the secretion of cytokines decreased, and the decrease was the most obvious in the HOP+H151-H group (P<0.05; Fig. 3D). qRT-PCR analysis revealed that the mRNA level of IL-6, TNF-α, and *IL-1β* in cells treated with HOP increased significantly (P<0.05), and H151 reduced this expression in a dose-dependent fashion, and the effect was the strongest in the HOP+H151-H group (P<0.05; Fig. 3E). Under safe concentrations, H151 can rely on hyperosmotic stress to increase the vitality of HCECs, reduce the damage of cell membranes, and inhibit the release of inflammatory cytokines.

H151 Inhibits Hyperosmotic Stress-Induced Overactivation of the cGAS–STING Pathway in Cells: WB analysis revealed that HOP cells exhibited markedly

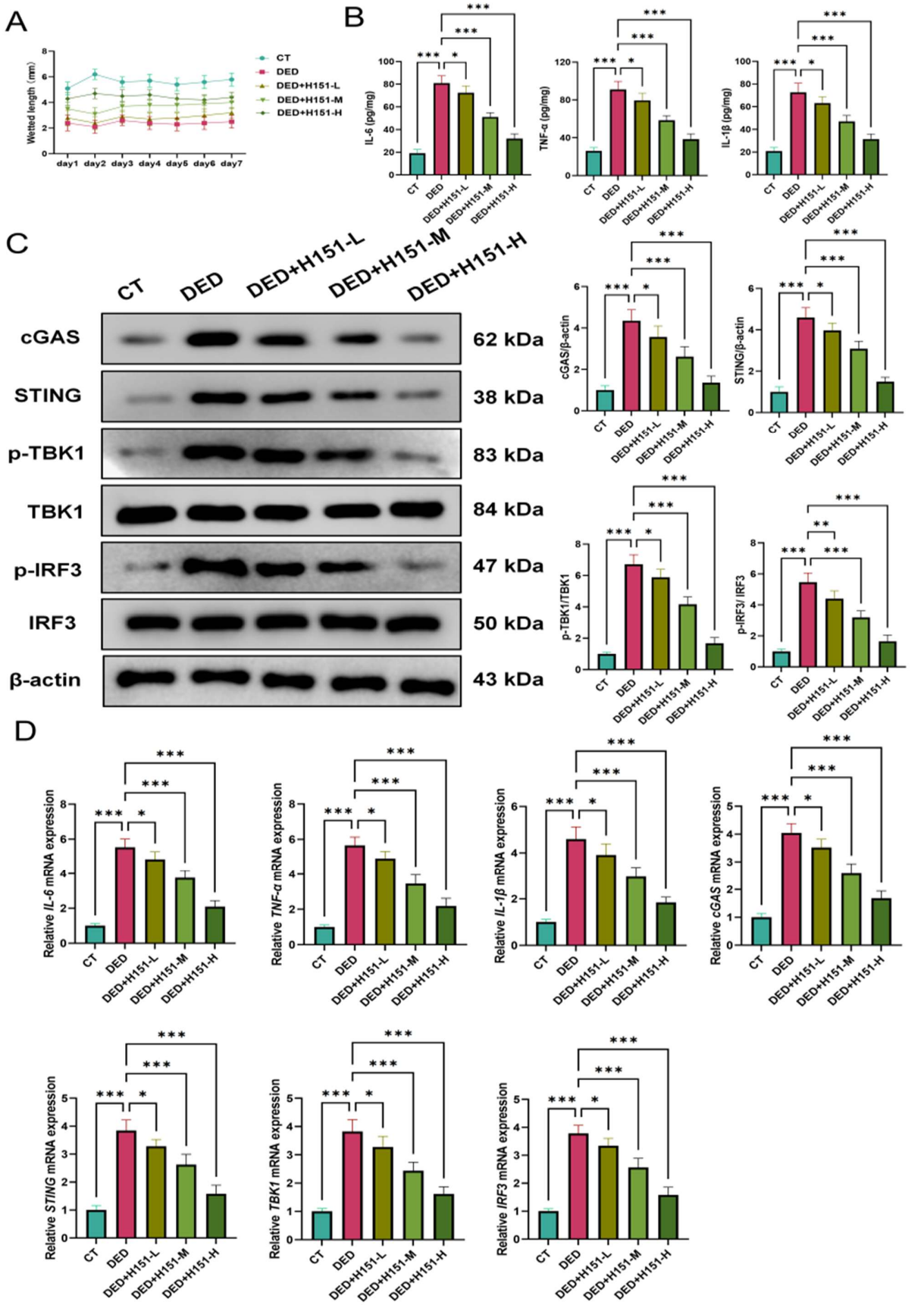

Fig. 1: H151 improves tear secretion and inhibits cGAS-STING pathway activation in DED mice. (A) Tear secretion measurement. (B) ELISA detection of inflammatory cytokines. (C) WB of cGAS-STING–related proteins. (D) qRT-PCR of corneal inflammatory cytokines and cGAS-STING genes. n=6; *P<0.05, **P<0.01, ***P<0.001 vs. DED group.

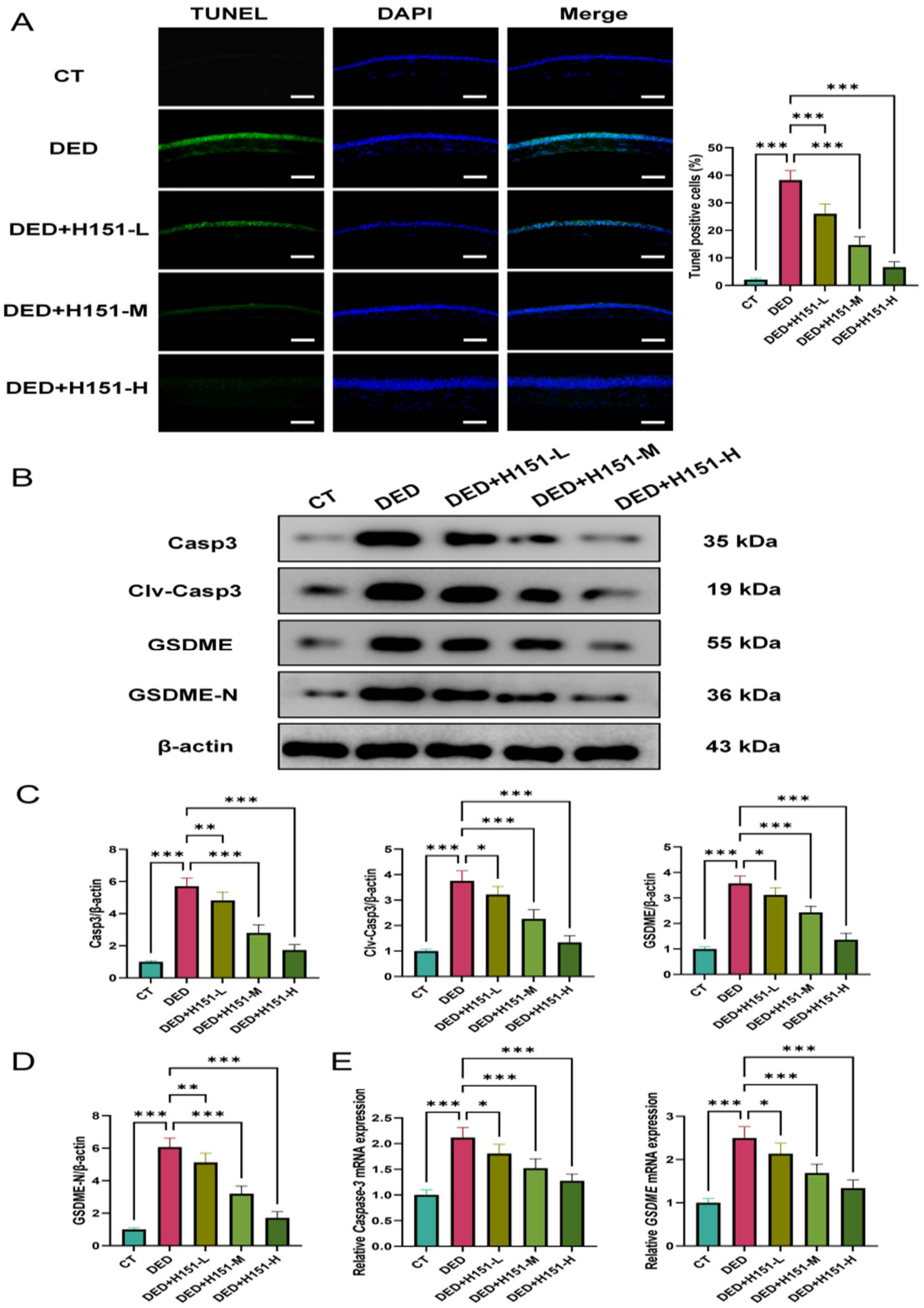

Fig. 2: H151 reduces corneal epithelial pyroptosis in DED mice by inhibiting the cGAS-STING pathway. (A) TUNEL staining (400×25μm). (B-D) WB analysis of pyroptosis-related protein expression in corneal tissues. (E) qRT-PCR analysis of pyroptosis-related mRNA levels in corneal tissues. n=6; *P<0.05, **P<0.01, ***P<0.001 vs. DED group.

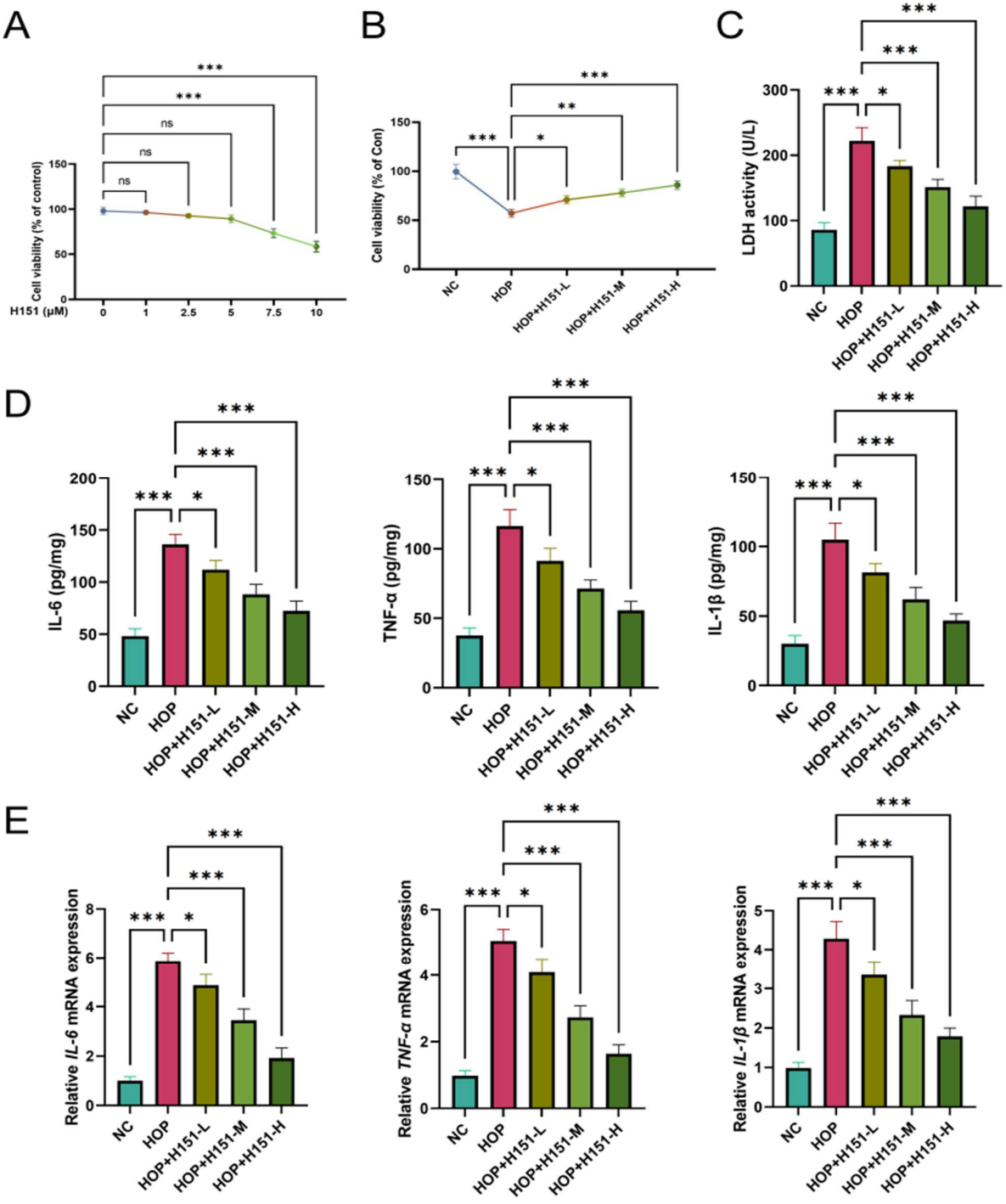

Fig. 3: Effects of H151 on cell viability, membrane damage, and inflammation in hyperosmotic-damaged cells. (A) Impact of varying H151 doses on cell viability. (B) Cell viability in each experimental group. (C) LDH release levels. (D) ELISA detection of cellular inflammatory cytokine levels. (E) qRT-PCR analysis of inflammatory cytokine gene expression. n = 3; *P<0.05, **P<0.01, ***P<0.001 vs. HOP group.

higher expression of cGAS–STING pathway proteins than the NC group (P<0.05), indicating that this pathway was activated under hyperosmotic stress (Figs. 4A and 4B). The application of H151 significantly reduced the protein levels of cGAS–STING pathway components in a concentration-dependent manner. The decrease is more obvious in the HOP+H151-H group (P<0.05; Figs. 4A and 4B). The trend obtained from qRT-PCR analysis matches the protein expression data. qRT-PCR analysis. Relative to the NC group, the mRNA levels of cGAS–STING related genes in HOP cells were markedly elevated (P<0.05). In the HOP+H151-H group, the mRNA expression of cGAS–STING–related genes was markedly reduced in a concentration-dependent manner following H151 treatment (P<0.05; Fig. 4C). Hyperosmotic stress obviously activates the cGAS–STING signaling pathway, while H151 can relieve this relatively high activation state.

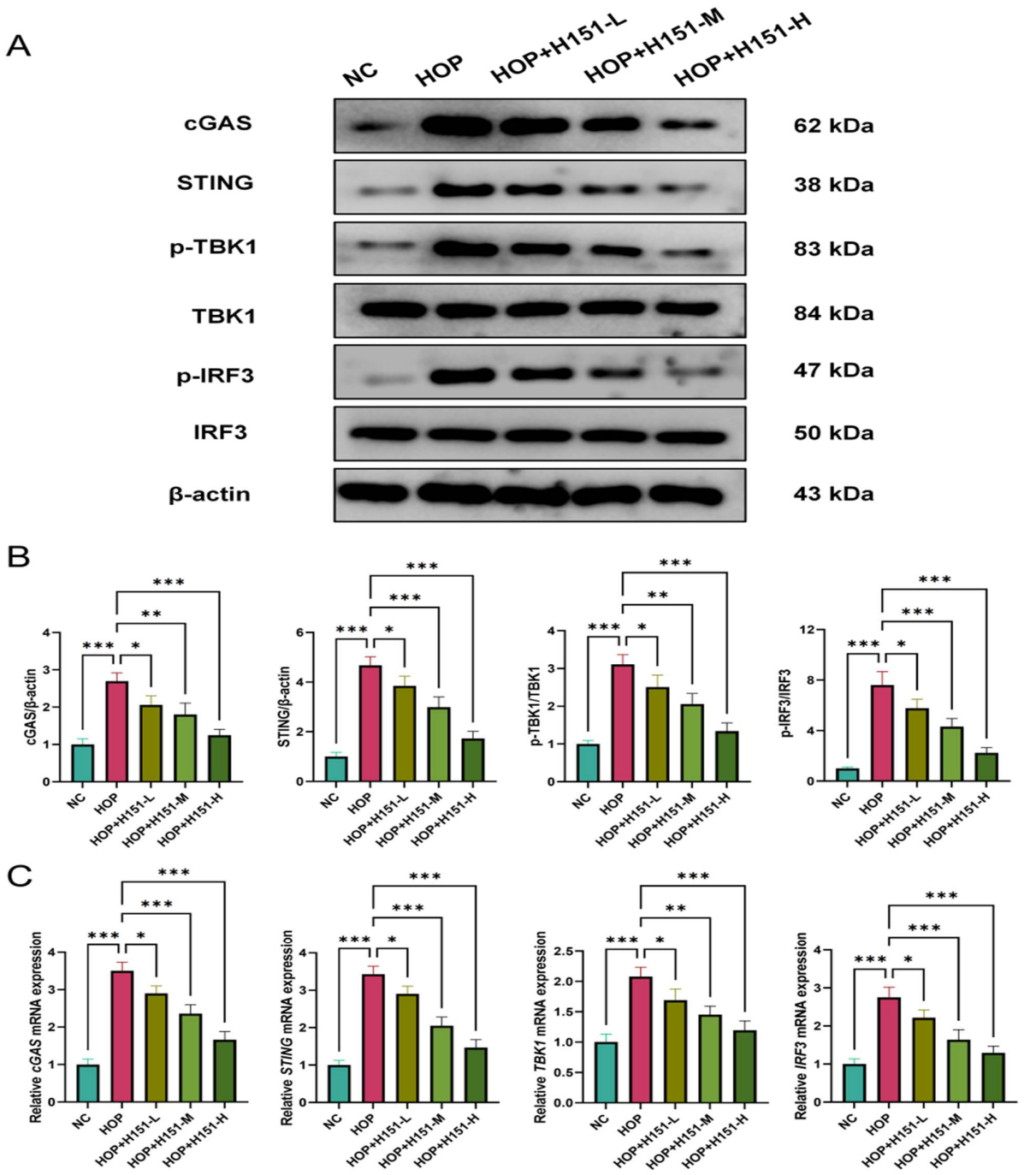

Fig. 4: Impact of H151 on cGAS-STING signaling in cells subjected to hyperosmotic stress. (A and B) WB analysis of cGAS-STING–related protein expression. (C) qRT-PCR analysis of cGAS-STING–related gene expression. n = 3; *P<0.05, **P<0.01, ***P<0.001 vs. HOP group.

H151 Inhibits Pyroptosis of Corneal Epithelial Cells Triggered by Hyperosmotic Stress: The number of TUNEL positive cells in the HOP group was markedly increased relative to the NC group (P<0.05), reflecting the situation of pyroptotic cell damage (Fig. 5A). The addition of H151 made the concentration of TUNEL positive cells decrease in a concentration-dependent fashion, and the effect of HOP + H151-H was the most obvious (P<0.05; Fig. 5A). WB analysis revealed that protein levels of caspase-3, cleaved caspase-3, GSDME, and its active fragment GSDME-N were significantly upregulated in HOP cells than in NC (P<0.05). H151 intervention substantially decreased the upregulation of these pyroptosis-related proteins in a dose-dependent fashion (Figs. 5B–5D). The findings of qRT-PCR analysis were consistent with the WB results, showing that hyperosmotic stress markedly increased *caspase-3* and *GSDME* mRNA levels (P<0.05), which were progressively reduced by H151 treatment, with the strongest inhibition observed in the HOP+H151-H group (P<0.05; Fig. 5E). The findings suggested that hyperosmotic stress markedly induced corneal epithelial cell pyroptosis, whereas H151 could suppress this effect in a dose-dependent manner.

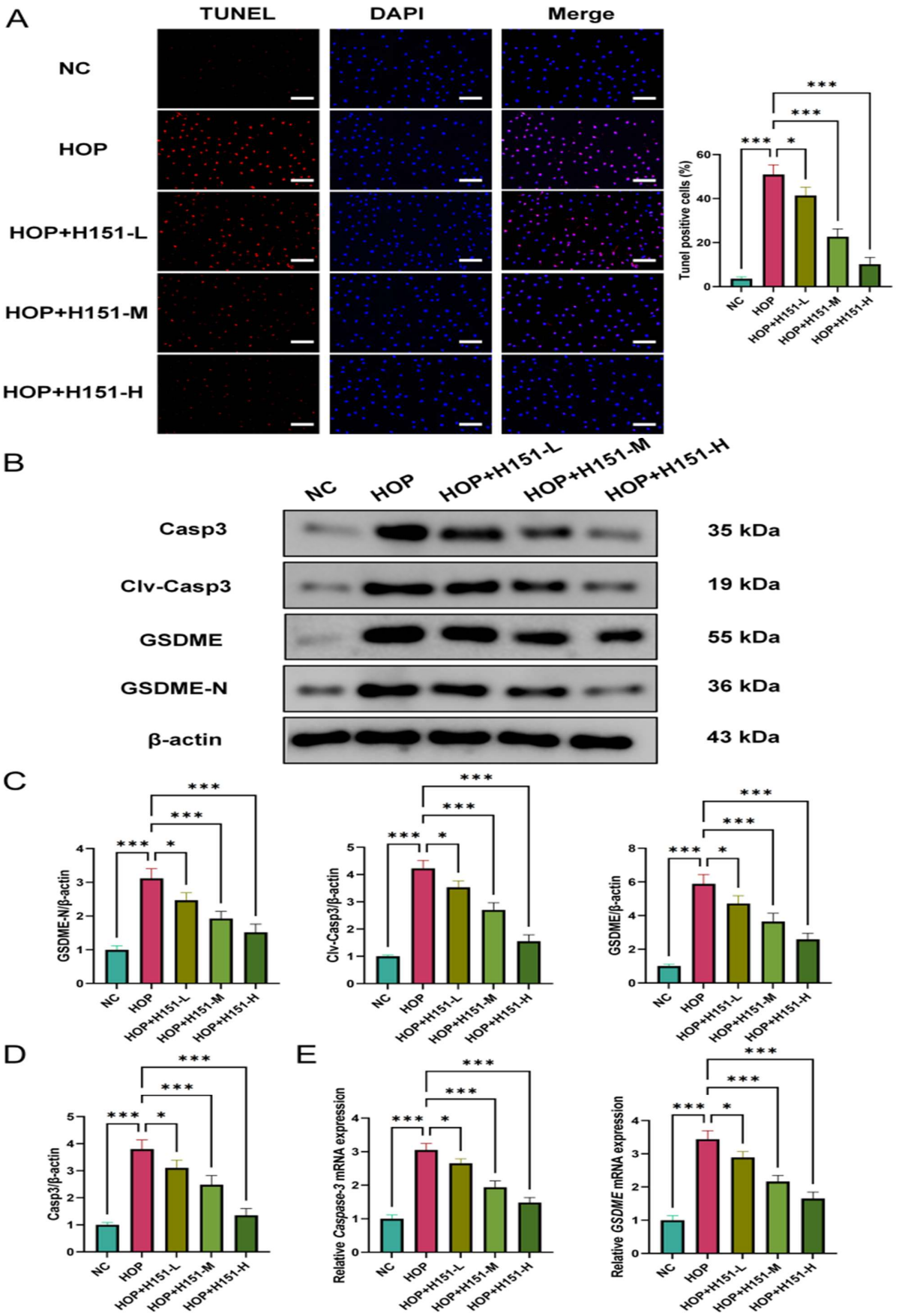

Fig. 5: Impact of H151 on corneal epithelial cell pyroptosis triggered by hyperosmotic stress. (A) TUNEL staining (200×50μm). (B-D) WB analysis of pyroptosis-related protein expression in cells. (E) qRT-PCR analysis of pyroptosis-related gene expression in cells. n=3; *P<0.05, ***P<0.001 vs. HOP group.

DISCUSSION

KCS in canines and felines, or DED in humans and animal models, is globally prevalent and often leads patients to seek ophthalmic care (Ling *et al*., 2021; Lu *et al*., 2022). In veterinary medicine, canine KCS is common, accounting for a large proportion of ophthalmic consultations in dogs, especially in immune-mediated and brachycephalic breeds, whereas feline KCS often occurs secondary to chronic conjunctivitis or feline herpesvirus infection (Wei *et al*., 2022; Chaithra *et al*., 2024; Picazo *et al*., 2024; Lau and Taylor, 2025). Apart from eye dryness, sensations of a foreign body, and visual tiredness, severe cases may experience vision loss, and chronic discomfort can even affect physical and mental health (Ax *et al*., 2023; Rolando *et al*., 2024). The pathogenesis of KCS is complex, with hyperosmotic stress, corneal damage, and inflammation as primary contributors (Chen *et al*., 2024; Hu *et al*., 2025). In dogs with KCS, chronic inflammation, impaired lacrimal gland function, and tear film instability can lead to sustained corneal epithelial damage (Jafari Taheri *et al*., 2025; Ohnishi *et al*., 2025). Inflammation of the corneal epithelium and immune cells disrupts cytokine production, further aggravating decreased tear production and destabilizing the tear film (Jeyabalan *et al*., 2023). Cat research shows that persistent ocular surface inflammation and virus reactivation can cause epithelial damage and disruption of tear film homeostasis (Colman *et al*., 2024).

Recently, pyroptosis has been recognized as a form of regulated cell death, distinct from apoptosis and secondary necrosis in both molecular mechanisms and morphological features. Apoptosis is generally characterized by caspase activation without plasma membrane rupture, whereas pyroptosis involves gasdermin-mediated membrane pore formation and inflammatory cytokine release. Secondary necrosis may occur when apoptotic cells are not efficiently cleared, leading to membrane rupture and inflammation, which may partially overlap with pyroptotic phenotypes. Research into the role of pyroptosis in inflammatory diseases is gradually increasing. It has the characteristics of cell swelling, plasma-membrane disruption accompanied by the liberation of pro-inflammatory cytokines (Wei *et al*., 2025). GSDME is a key execution protein, which can be cleaved by caspase-3 to promote pyroptosis (Du *et al*., 2024). In the present study, in vivo DED mouse models and in vitro hyperosmotic - stressed corneal epithelial cells exhibited a significant upregulation of caspase-3 and GSDME at the levels of both mRNA and protein. The observed TUNEL positivity and caspase-3 activation may reflect a spectrum of regulated cell death processes, including apoptosis, pyroptosis-like cell death, and potentially secondary necrosis. While these features are not exclusively specific to pyroptosis, the concomitant upregulation and cleavage of GSDME suggest a shift toward pyroptosis-like characteristics rather than classical apoptosis alone. This indicates the involvement of the caspase-3/GSDME axis in mediating corneal epithelial pyroptosis during KCS. Notably, the upregulation of caspase-3 usually exceeds the levels of GSDME. Although direct evidence of caspase-3/GSDME-mediated corneal pyroptosis is currently lacking in felines and is rarely observed in canines, related mechanisms have been documented. A similar pyroptotic tendency in canines was demonstrated by Wang *et al*. (2024), who reported that the expression of NLRP3 and gasdermin D (GSDMD) proteins increases significantly in infected corneas, indicating that pyroptosis participates in canine ocular surface inflammation. In cats, chronic viral keratoconjunctivitis has also been associated with epithelial and stromal inflammatory cell activation, suggesting that inflammasome-related pathways may contribute to feline ocular surface damage (Sebbag *et al*., 2021). Although there is no direct evidence linking these species-specific differences to epigenetic regulation or variations in natural cleavage sites of GSDME in corneal epithelial cells or DED conditions, previous studies in tumor tissues have shown that GSDME can be silenced via promoter methylation or lose function due to cleavage site mutations (e.g., D270A/D273A), thereby impairing caspase-3-mediated pyroptosis (Li *et al*., 2022).

The cGAS–STING pathway functions as a crucial intracellular DNA-sensing signaling cascade, whose activation induces type I interferons (such as IFN-β) and pro-inflammatory cytokines (including IL-6) through the TBK1–IRF3 axis (Cheng *et al*., 2020). Extensive studies have shown that overactivation of this pathway is linked to cell damage and chronic inflammation in various immune and inflammatory diseases. For instance, abnormal activation of cGAS–STING has been identified as a major regulator of disease progression in systemic lupus erythematosus, Sjögren's syndrome, and psoriasis (Chang *et al*., 2024; Xu *et al*., 2024; Zu *et al*., 2024).

Evidence shows that the cGAS–STING signaling pathway is involved in various types of programmed cell death, including apoptosis, necroptosis, and pyroptosis (Zheng *et al*., 2023). The production of pro-inflammatory cytokines and the pathological activity in pyroptosis and ocular/retinal diseases are related, which can exacerbate ocular surface injury (Shang *et al*., 2025). H151-mediated STING inhibition can effectively suppress the activity of the cGAS–STING pathway, thereby reducing the inflammatory response and cell damage (Sun *et al*., 2025). Our research results initially suggest that, in the context of DED, activation of the cGAS - STING axis may lead to pyroptosis in corneal epithelial cells and potentially trigger inflammatory responses. H151 can increase tear secretion, reduce damage to corneal epithelium, and, in a dose-dependent manner, inhibit the expression of genes and proteins associated with pyroptosis, with the most obvious effect at the highest concentration. Through TUNEL staining, it was found that H151 can reduce DNA fragmentation in corneal epithelial cells, which reflects alleviation of regulated cell death but cannot distinguish pyroptosis from apoptosis or secondary necrosis. Ultrastructural analyses, such as membrane ballooning by electron microscopy, and detection of inflammasome-related markers (e.g., NLRP3, ASC) were not performed; thus, pyroptosis identification is mainly based on molecular signatures, limiting definitive morphological confirmation. Although the cGAS–STING pathway has not been fully studied in dogs and cats, there may be similar inflammatory signaling mechanisms in diseases such as canine chronic dacryoadenitis and feline virus-related conjunctivitis (Wang *et al*., 2023). The research showed that excessive activation of the cGAS–STING pathway is very crucial in the pathogenesis of DED, and targeting this axis may be an effective therapy.

In the DED model, inflammatory cytokines—including IL-6, TNF-α, and IL-1β—exhibit a markedly elevated level, and H151 administration can make their expression weaken. The results show that pyroptosis and inflammation can form a self-amplifying loop, and cytokines are released through GSDME pores to promote local inflammation (Li *et al*., 2021). Therefore, GSDME is a mediator of corneal epithelial cell pyroptosis and an important regulatory factor in the inflammatory signaling network.

However, this study has several limitations. First, the role of GSDME as the principal executioner of pyroptosis in DED has not been fully established. Second, although pharmacological inhibition of STING using H151 consistently attenuated inflammatory responses and cell death, genetic approaches such as siRNA- or CRISPR-mediated knockdown of cGAS or STING were not employed. Therefore, the direct causal contribution of individual components of the cGAS–STING pathway to caspase-3/GSDME activation cannot be conclusively determined. Future studies incorporating genetic loss-of-function strategies will be necessary to validate the mechanistic hierarchy proposed here. In addition, KCS is common in dogs, and ocular surface inflammation is prevalent in cats, suggesting that investigation of this signaling axis in companion animals may provide valuable comparative and translational insights. However, the present findings are derived exclusively from murine models and human corneal epithelial cells, and species-specific validation—ideally involving additional animal models and clinical samples—will be required before extrapolating these mechanisms to veterinary patients.

Conclusions: This study explores the association between cGAS–STING activation and GSDME-related pyroptosis-like cell death in the pathogenesis of DED. In the DED model, the expression of caspase-3 and GSDME was significantly upregulated, indicating their involvement in corneal epithelial cell pyroptosis. Overactivation of the cGAS–STING pathway amplifies inflammatory responses and exacerbates epithelial damage. H151 pharmacological inhibition can effectively restore tear secretion, alleviate corneal inflammation, and inhibit pyroptosis activity in a dose-dependent manner. These findings offer fresh perspectives on the contribution of pyroptosis to the pathogenesis of DED and provide potential avenues for targeted therapeutic intervention.

Competing interests: No conflict of interest exits in this manuscript

Authors contribution: Haishu Dong designed the study, performed the experiments, analyzed the data, and wrote the manuscript. Jiawei Chen contributed to the experimental design, data analysis, and manuscript revision. Jian Sun and Yi Wu performed the in vitro experiments and assisted with data interpretation. Zipei Jiang and Jiayu Zhang supervised the study, contributed to the study design, and critically revised the manuscript. All authors approved the final version of the manuscript.

Funding: This work was supported by the Science and Technology Program of Wenzhou (GK20250116).

REFERENCES

Al-Mohtaseb Z, Schachter S, Shen Lee B, *et al*., 2021. The relationship between dry eye disease and digital screen use. Clinical Ophthalmology 15:3811–3820.

Almulhim A, 2024. Therapeutic targets in the management of dry eye disease associated with Sjögren's syndrome: An updated review of current insights and future perspectives. Journal of Clinical Medicine 13:1777.

Avci N, Gumus F, Boztok Ozgermen B, *et al*., 2025. Keratoconjunctivitis sicca in intact Aksaray Malakli breed dogs: Evaluation of 50 cases. Veterinary Ophthalmology 28:802–811.

Ax T, Ganse B, Fries FN, *et al*., 2023. Dry eye disease in astronauts: A narrative review. Frontiers in Physiology 14:1281327.

Chaithra SN, Gopinathan A, Singh K, *et al*., 2024. Epidemiological insights into keratoconjunctivitis sicca (KCS) in canine populations: a study in brachycephalic breeds. Journal of Experimental Zoology India 27(2).

Chang L, 2024. Harnessing cGAS-STING axis for therapeutic benefits in systemic lupus erythematosus. International Journal of Rheumatic Diseases 27:e15256.

Chen TG, Zhou N, Liang Q, *et al*., 2024. Biochanin A: Disrupting the inflammatory vicious cycle for dry eye disease. European Journal of Pharmacology 977:176583.

Cheng ZL, Dai T, He XL, *et al*., 2020. The interactions between cGAS-STING pathway and pathogens. Signal Transduction and Targeted Therapy 5:91.

Du L, Ming HY, Yan ZN, *et al*., 2024. Decitabine combined with cold atmospheric plasma induces pyroptosis via the ROS/Caspase-3/GSDME signaling pathway in Ovcar5 cells. Biochimica et Biophysica Acta – General Subjects 1868:130602.

Fischer FA, Chen KW and Bezbradica JS, 2021. Posttranslational and therapeutic control of gasdermin-mediated pyroptosis and inflammation. Frontiers in Immunology12:661162.

Gu XT, Chen Y, Cao KY, *et al*., 2024. Therapeutic landscape in systemic lupus erythematosus: mtDNA activation of the cGAS-STING pathway. International Immunopharmacology 133:112114.

Han YP, Qiu LC, Wu HX, *et al*., 2024. Focus on the cGAS-STING signalling pathway in sepsis and its inflammatory regulatory effects. Journal of Inflammation Research 17:3629–3639.

Hu JY, Zeng YM, Tang LY, *et al*., 2025. Topical application of VitB6 ameliorates PM2.5-induced dry eye via NFκB pathway in a murine model. Biomedicines 13:541.

Hu R, Shi J, Xie CM, *et al*., 2025. Dry eye disease: Oxidative stress on ocular surface and cutting-edge antioxidants. Global Challenges 9:e00068.

Jafari Taheri M, Bitaraf M, Behtari M, *et al*., 2025. Clinical outcomes of stem cell therapy in dogs with keratoconjunctivitis sicca: A systematic review and meta-analysis. Veterinary Ophthalmology (ahead of print).

Jeyabalan N, Pillai AM, Khamar P, *et al*., 2023. Autophagy in dry eye disease: Therapeutic implications of autophagy modulators on the ocular surface. Indian Journal of Ophthalmology 71:1285–1291.

Kontoh-Twumasi R, Aliste A, Scheid A, *et al*., 2025. L-carnitine restores adherens junction integrity and promotes wound healing in corneal epithelial cells exposed to hyperosmolar stress. Experimental Eye Research 258:110499.

Lau WI, Taylor RM, 2025. Prevalence of corneal disorders in pugs attending primary care veterinary practices in Australia. Animals 15:531.

Li HQ, Wang X, Yu LJ, *et al*., 2022. Duck gasdermin E is a substrate of caspase-3/7 and an executioner of pyroptosis. Frontiers in Immunology 13:1078526.

Li JN, Bao XR, Guo SJ, *et al*., 2024. Cell death pathways in dry eye disease: Insights into ocular surface inflammation. Ocular Surface 34:535–544.

Li YS, Yuan Y, Huang ZX, *et al*., 2021. GSDME-mediated pyroptosis promotes inflammation and fibrosis in obstructive nephropathy. Cell Death and Differentiation 28:2333–2350.

Liao K, Zeng H, Yang X, *et al*., 2024. KCNK5 regulates potassium efflux and induces pyroptosis in corneal epithelial cells through TNFSF10-mediated autophagy in dry eye. Investigative Ophthalmology & Visual Science 65:34.

Ling JW, Chan BC, Tsang MS, *et al*., 2021. Current advances in mechanisms and treatment of dry eye disease: Toward anti-inflammatory and immunomodulatory therapy and traditional Chinese medicine. Frontiers in Medicine 8:815075.

Lu XF, Li J, Ye SH, *et al*., 2022. Acupuncture for dry eye disease after recovery from COVID-19: Protocol for systematic review. Medicine 101:e31234.

Ohnishi A, Takeda S, Okada Y, *et al*., 2025. Risk factors for radiation-induced keratoconjunctivitis sicca in dogs treated with hypofractionated intensity-modulated radiation therapy for intranasal tumors. Animals 15(15):2258.

Ouyang WJ, Wang SB, Yan D, *et al*., 2023. cGAS-STING-dependent sensing of mtDNA mediates ocular surface inflammation. Signal Transduction and Targeted Therapy 8:371.

Papas EB, 2021. The global prevalence of dry eye disease: A Bayesian view. Ophthalmic and Physiological Optics 41:1254–1266.

Picazo RA, Rojo C, Rodriguez-Quiros J, *et al*., 2024. Advances in mesenchymal stem cell therapies for wounds and ocular and neuromuscular diseases in companion animals. Animals 14:1363.

Qian YX, Cao SJ, He L, *et al*., 2025. Activation of the cGAS-STING pathway mediated by nanocomplexes for tumor therapy. Current Pharmaceutical Design 31:1604–1618.

Rolando M, Arnaldi D, Minervino A, *et al*., 2024. Dry eye in mind: Relationship between sleep and ocular surface diseases. European Journal of Ophthalmology 34:1128–1134.

Roszkowska AM, Polito F, Wierzbowska J, *et al*., 2025. Curcumin-liposome formulation suppresses inflammatory cascade activated by oxidative stress in human corneal epithelial cells. Experimental Eye Research 260:110584.

Sebbag L, Thomasy SM, Leland A, *et al*., 2021. Altered corneal innervation and ocular surface homeostasis in FHV-1-exposed cats: A preliminary study suggesting metaherpetic disease. Frontiers in Veterinary Science 7:580414.

Shang ZL, Qin D, Liu XG, *et al*., 2025. The cGAS-STING pathway in age-related ocular diseases: Mechanisms and therapeutic opportunities. Cellular Signalling 135:112069.

Shimizu S, Sato S, Taniguchi H, *et al*., 2021. Observation of chronic graft-versus-host disease mouse cornea with in vivo confocal microscopy. Diagnostics 11:1515.

Song JP, Dong H, Wang TT, *et al*., 2024. Impact of microbiota on dry eye: A review of the gut-eye axis. BMC Ophthalmology 24:262.

Sun X, Zhang JY, Li XX, *et al*., 2025. Fenofibrate inhibits activation of cGAS-STING pathway by reducing mitochondrial damage in diabetic dry eye. Free Radical Biology and Medicine 235:364–378.

Wang J, Li M, Li M, 2023. Newcastle disease virus LaSota strain induces apoptosis and activates the TNFα/NF-κB pathway in canine mammary carcinoma cells. Veterinary and Comparative Oncology 21:520–532.

Wang L, Tian Y, Zhang H, *et al*., 2025. Caspase-3/GSDME-mediated corneal epithelial pyroptosis promotes dry eye disease. Investigative Ophthalmology & Visual Science 66:24.

Wang Z, Guo L, Yuan C, *et al*., 2024. Staphylococcus pseudintermedius induces pyroptosis of canine corneal epithelial cells via ROS-NLRP3 pathway. Virulence 15:1–12.

Wei LN, Wu CH, Lin CT, *et al*., 2022. Topical applications of allogeneic adipose-derived mesenchymal stem cells ameliorate the canine keratoconjunctivitis sicca. BMC Veterinary Research 18(1):217.

Wei XR, Ran SD, Yan XR, *et al*., 2025. Pyroptosis in pulpitis. Journal of Inflammation Research 18:5867–5879.

Xu JB, Chen CY, Yin JH, *et al*., 2023. Lactate-induced mtDNA accumulation activates cGAS-STING signalling in Sjögren's syndrome. International Journal of Medical Sciences 20:1256–1271.

Xu TT, Zhong XJ, Luo NN, *et al*., 2024. Cytosolic DNA in AIM2 and cGAS-STING-mediated psoriasis development. Clinical, Cosmetic and Investigational Dermatology 17:2345–2357.

Yang YT, Huang YM, Zeng ZG, 2022. Advances in cGAS-STING signalling pathway and diseases. Frontiers in Cell and Developmental Biology 10:800393.

Zhang ZX, Wei X, Huang Q, *et al*., 2025. STING antagonists targeting cGAS-STING pathway alleviate psoriasis-like dermatitis. European Journal of Pharmaceutical Sciences 210:107091.

Zheng WL, Liu AJ, Xia NW, *et al*., 2023. How innate immune DNA sensing via cGAS-STING is involved in apoptosis. International Journal of Molecular Sciences 24:3029.

Zhong HH, Chen GJ, Li T, *et al*., 2023. Nanodrug augmenting antitumor immunity via pyroptosis and cGAS-STING activation for TNBC therapy. Nano Letters 23:5083–5091.